NANO LETTERS

2005
Vol. 5, No. 7
1407−1411

General Synthesis of Manganese-Doped II–VI and III–V Semiconductor Nanowires

Pavle V. Radovanovic,[†] Carl J. Barrelet,[†] Silvija Gradečak,[†] Fang Qian,[†] and Charles M. Lieber*[,†,‡]

Department of Chemistry and Chemical Biology, Harvard University, 12 Oxford Street, Cambridge, Massachusetts 02138, and Division of Engineering and Applied Sciences, Harvard University, Cambridge, Massachusetts 02138

Received April 22, 2005; Revised Manuscript Received May 26, 2005

ABSTRACT

A general approach for the synthesis of manganese-doped II–VI and III–V nanowires based on metal nanocluster-catalyzed chemical vapor deposition has been developed. High-resolution transmission electron microscopy and energy-dispersive X-ray spectroscopy studies of Mn-doped CdS, ZnS, and GaN nanowires demonstrate that the nanowires are single-crystal structures and homogeneously doped with controllable concentrations of manganese ions. Photoluminescence measurements of individual Mn-doped CdS and ZnS nanowires show characteristic pseudo-tetrahedral Mn^{2+} ($^4T_1 \rightarrow {}^6A_1$) transitions that match the corresponding transitions in bulk single-crystal materials well. Photoluminescence studies of Mn-doped GaN nanowires suggest that manganese is incorporated as a neutral (Mn^{3+}) dopant that partially quenches the GaN band-edge emission. The general and controlled synthesis of nanowires doped with magnetic metal ions opens up opportunities for fundamental physical studies and could lead to the development of nanoscale spintronic devices.

Semiconductor nanowires are emerging as versatile building blocks for nanoscale electronic and photonic devices[1,2] ranging from electronic sensors[3] to nanoscale light-emitting diodes.[4,5] The ability to utilize a bottom-up paradigm to assemble distinct types of building blocks into different functional devices is especially important because it represents an approach to active devices and systems that contrasts with conventional technologies.[1] The potential uniqueness of the bottom-up approach thus rests in part on the diversity of functional building blocks available for assembly, and in this regard, researchers have made many advances.[1,2] For example, basic semiconductor nanowires have been elaborated through the controlled introduction of simple dopants, which have enabled the demonstration of electronically well-defined materials essential for studies of active electronic and photonic devices.[3−5]

Substitutional doping of semiconductors with paramagnetic transition-metal ions can produce magnetic materials called dilute magnetic semiconductors (DMSs).[6] The interesting magnetic and magneto-optical properties of DMSs, which arise from spin-exchange interactions between the dopant ions and the semiconductor charge carriers (sp−d exchange interactions), have been the focus of intense efforts for conventional planar semiconductor structures because of the possibility of utilizing these materials for semiconductor spin-based electronics or spintronics.[7,8] Much less attention has been placed on doping nanostructures with paramagnetic metal ions, although clear evidence for cobalt- and manganese-doped nanocrystals of different group II−VI materials has been obtained.[9−11]

More recently, Mn-doped nanowires have been prepared using several different synthetic methods.[12−14] ZnO nanowires doped with Mn ions were achieved by ion implantation followed by thermal annealing to remove defects introduced during the implantation step.[13] In cases where nanowire structures are robust to thermal annealing, this approach has considerable promise for controlled transition-metal-ion doping. Alternatively, chemical vapor deposition methods have been used to provide evidence for the direct growth of Mn-doped GaN nanowires.[12,14] Here we report the general synthesis of single-crystalline II−VI and III−V DMS nanowires using Mn-doped CdS, ZnS, and GaN nanowires as examples. The ability to synthesize well-defined and synthetically tunable DMS nanowire materials could open up new opportunities for fundamental studies of spin interactions in quasi-1D systems as well as provide new building blocks for spintronics.

Mn-doped nanowires were prepared by adapting metal nanocluster-catalyzed chemical vapor deposition (CVD)

* Corresponding author. E-mail: cml@cmliris.harvard.edu.
[†] Department of Chemistry and Chemical Biology, Harvard University.
[‡] Division of Engineering and Applied Sciences, Harvard University.

10.1021/nl050747t CCC: $30.25
Published on Web 06/17/2005

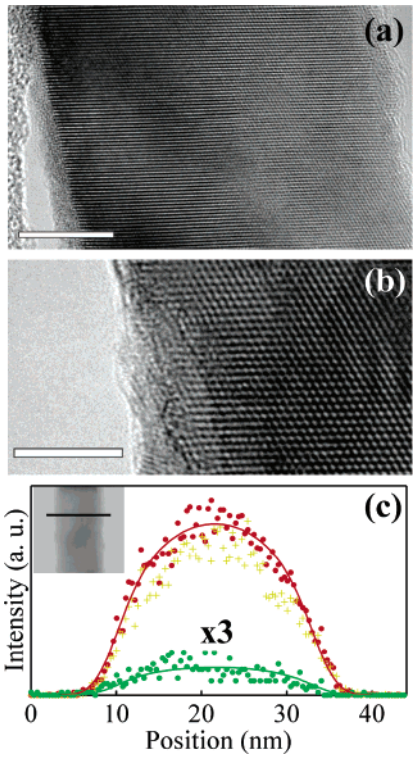

Figure 1. (a) TEM image of a 7% Mn-doped CdS nanowire, (b) HREM image of the same nanowire, and (c) EDX line scans for the nanowire shown in the inset, with Cd, S, and Mn data plotted as red dots, yellow crosses, and green dots, respectively. The red and green solid lines through the data are fits to the experimental data for Cd and Mn, respectively. Scale bars in a and b are 10 and 5 nm, respectively.

methods for II−VI[15] and III−V[5] nanowire growth. The synthesis of Mn-doped CdS (Mn:CdS) and ZnS (Mn:ZnS) nanowires was carried out using a core/shell methodology. First, CdS and ZnS nanowires were synthesized using gold nanocluster-catalyzed vapor−liquid−solid (VLS) growth with single-source $Cd(S_2CNEt_2)_2$ and $Zn(S_2CNEt_2)_2$ precursors, respectively.[15] Second, shell layers were grown at lower temperature using either a mixture of $Cd(S_2CNEt_2)_2$ and $Mn_2(CO)_{10}$ (molar ratio: $n(Cd)/n(Mn) = 10/1$) or $Zn(S_2CNEt_2)_2$ and $MnCO_3$ (molar ratio: $n(Zn)/n(Mn) = 5/1$) as precursors. The shells were grown at 400 °C for Mn:CdS and at 500 °C for Mn:ZnS nanowires. Doping concentrations were systematically varied by changing the Mn/Cd or Mn/Zn precursor ratio and the shell thickness. Following shell growth, the nanowires were annealed at ca. 250 °C for 2 h. The synthesis of Mn-doped GaN (Mn:GaN)NWs was carried out in a single step from a mixture of elemental Ga and up to 10 mol % $MnCl_2$ in a flow of NH_3 and H_2 using a nickel catalyst prepared in situ.[5]

The Mn-doped nanowires were characterized at the single-nanowire level using transmission electron microscopy (TEM), energy-dispersive X-ray (EDX) spectroscopy, and photoluminescence.[16] A representative TEM image of a Mn:CdS nanowire (Figure 1a) shows that these nanowires have smooth surfaces and uniform thicknesses along the growth direction. From the average values of the nanowire diameters before and after the shell growth, we estimate that the diameter of the initial nanowire core in Figure 1a is about 20 nm and that the shell thickness is ca. 7 nm, where the core diameter is consistent with that obtained using 20-nm-diameter gold nanoclusters in a VLS process.[15] In addition, the absence of defects or boundaries related to a core/shell interface in the TEM data suggests that the Mn-doped CdS shell grows epitaxially. High-resolution TEM (HRTEM) images (Figure 1b) confirm that shell growth is epitaxial; moreover, measurements made at different positions along the lengths of a number of Mn:CdS nanowires show that these single-crystal materials do not have observable secondary phases. Previous TEM studies of Mn-doped thin film semiconductors have demonstrated the importance of such studies for identifying Mn-rich phases.[17] Because Mn-rich phases can significantly affect measured physical properties, our HRTEM images are important in showing that the Mn:CdS nanowires are homogeneously doped at this level of characterization. Similar TEM characterization studies and results have been obtained for the Mn:ZnS nanowires. Specifically, TEM, HRTEM, and electron diffraction data recorded on Mn:ZnS nanowires prepared by the core/shell approach (Figure S1, Supporting Information) show that the nanowires have single-crystal structures without evidence for secondary phases.

In addition, EDX measurements were carried out to determine the overall composition and spatial distribution of Mn ions in individual nanowires. EDX measurements on a representative Mn:CdS nanowire (Figure 1c) show that the Mn composition is ca. 7%. More importantly, the Mn, Cd, and S elemental line scans recorded perpendicular to the nanowire axis are all of similar functional form. This similarity in Mn and Cd EDX profiles was quantified by modeling.[18−20] Significantly, our analysis shows that the Cd and Mn elemental line scans are well fit to the same function (solid lines, Figure 1c), thus indicating that the Mn ions are distributed homogeously through the nanowire and not localized in an outer shell. To test this interpretation further, we also modeled the Mn EDX line scan profile assuming that dopant ions are located exclusively in a shell. This analysis (Figure S2, Supporting Information) shows that the maximum Mn signal should occur at the edges of the nanowire, where the Cd intensity is dropping rapidly, and that the Mn signal should exhibit a dip at the center of the nanowire, where the Cd signal is a maximum. Notably, this scenario clearly contrasts the observed experimental data and thus supports our conclusion that Mn:CdS nanowires are homogeneously doped. During synthesis, the Mn is added formally as a shell to a CdS nanowire core; however, fast diffusion, which has been documented for first-row transition-metal elements in II−VI lattices at comparable temperatures,[21] can explain the observed homogeneous Mn ion distribution in the Mn:CdS nanowires.

The Mn-doped CdS and ZnS nanowires were also characterized at the single-nanowire level using photoluminescence (PL) measurements. A representative PL spectrum recorded on a single Mn:CdS nanowire at 5 K (Figure 2a) excited at 395 nm exhibits two distinct features centered at 495 and 570 nm. The relatively narrow (17 nm full-width at

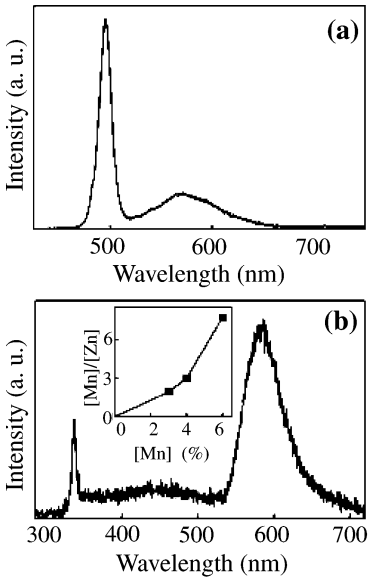

Figure 2. (a) PL spectrum of a single Mn-doped CdS nanowire at 5 K and (b) PL spectrum of a Mn-doped ZnS nanowire at 300 K. The Mn concentrations determined by EDX for the Mn:CdS and Mn:ZnS samples were ca. 7 and 3%, respectively.

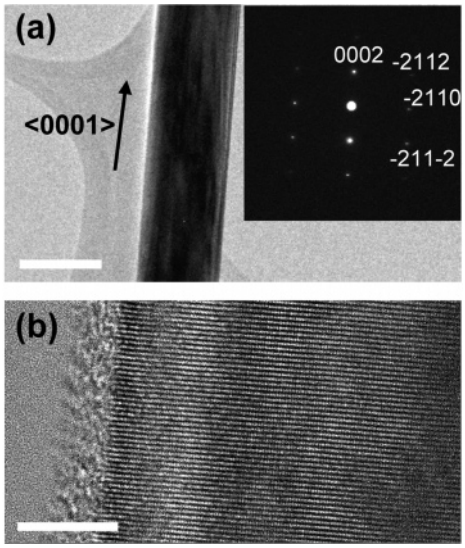

Figure 3. (a) TEM image of an ca. 2% Mn-doped GaN nanowire with a hexagonal cross section. (Inset) Electron diffraction pattern indexed for the wurtzite structure with a ⟨0001⟩ growth direction. (b) HRTEM image of the same nanowire. The electron diffraction and HRTEM were recorded along the [01-10] zone axis. Scale bars in a and b are 200 and 5 nm, respectively.

half-maximum) peak at 495 nm corresponds to CdS nanowire band-edge emission.[22] A comparison of PL spectra recorded from similarly sized Mn:CdS and CdS nanowires under the same conditions shows that the presence of Mn dopant ions leads to a partial quenching of the CdS band-edge emission, which is consistent with energy transfer to Mn ions in the lattice (see below). Significantly, the good agreement of the second feature centered at 570 nm with PL data from single-crystal and nanocrystalline Mn:CdS[23−25] enables the assignment of this peak to the Mn^{2+} $^4T_1 \rightarrow {}^6A_1$ d−d ligand-field transition. This spectral feature is characteristic of isolated Mn^{2+} in a quasi-tetrahedral site[26] and together with the EDX measurements described above (Figure 1c) is a clear indication of homogeneous (not surface) incorporation of isolated Mn ions.

In addition, PL studies of Mn:ZnS nanowires were carried out. A typical PL spectrum recorded from a single Mn:ZnS nanowire at 300 K (Figure 2b) shows features centered at 337 and 585 nm. The sharp feature at 337 nm corresponds to band-edge emission from the ZnS nanowire, whereas the feature at 585 nm can be assigned to the $^4T_1 \rightarrow {}^6A_1$ transition in Mn^{2+}.[27] In the case of Mn:ZnS nanowires, the Mn^{2+}-based emission is dominant with respect to the band-edge emission. This suggests that energy transfer to Mn^{2+} in ZnS is more efficient than in CdS nanowires. To clarify further energy transfer, we have characterized the relative Mn^{2+} $^4T_1 \rightarrow {}^6A_1$ to ZnS band-edge emission intensity as a function of concentration of Mn ions. These data (inset, Figure 2b) show that the ratio increases almost linearly up to 6% Mn, and further support the conclusion that the Mn-doped nanowires have uniform distribution of isolated paramagnetic ions.

We have explored the generality of our approach to Mn-doped nanowires through studies of Mn:GaN, which is a potentially attractive system because of the prediction for ferromagnetic ordering above room temperature.[28] TEM and electron diffraction data obtained from a ca. 2% Mn-doped GaN nanowire (Figure 3a) show that the nanowire is a single crystal with wurtzite structure and a ⟨0001⟩ growth axis; additional TEM images also demonstrate that the nanowire has a hexagonal cross section. A representative HRTEM image of the same nanowire (Figure 3b) further illustrates the single-crystalline structure and the lack of secondary phases, which are often encountered in the synthesis of Mn-doped III−V thin films using gas-phase deposition techniques.[17] We emphasize that the same high-quality single-crystal Mn:GaN structures have been observed in detailed analyses of at least 10 independent samples prepared in different growth runs using similar experimental conditions. These results testify to the reproducibility of the Mn:GaN nanowires prepared in our studies. In addition, we note that ca. 15% of Mn:GaN nanowires have triangular cross sections; in contrast, the growth of pure GaN under the same conditions yields almost exclusively nanowires with hexagonal cross sections. These results suggest that it will be interesting in the future to explore further how reactant species might be used to control faceting in VLS-based nanowire growth.

The concentration and distribution of Mn dopants were characterized by EDX as discussed above for Mn:CdS and Mn:ZnS nanowires. EDX elemental line scans recorded from single Mn:GaN nanowires with hexagonal and triangular cross sections are shown in parts a and b of Figure 4, respectively. An inspection of the data shows for both nanowire morphologies that the Ga (K shell, 9.25 keV) and Mn (K shell, 5.9 keV) elemental profiles have a similar functional form, which suggests that the Mn dopants are incorporated homogeneously through the nanowire structure. Quantitative modeling[18−20] of the Ga and Mn EDX profiles demonstrates that the Ga and Mn elemental line scans are fit by the same scaled function (solid lines, Figure 4) for both the hexagonal

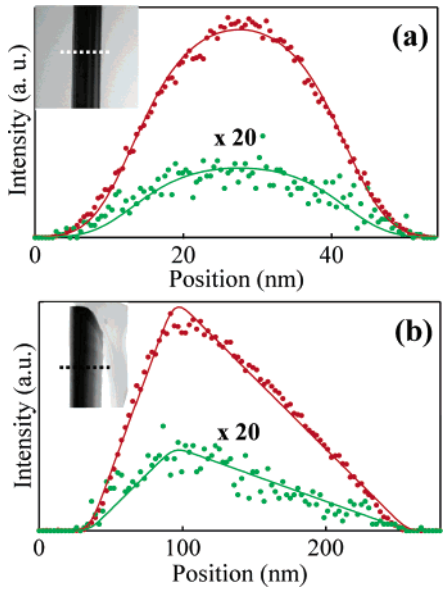

Figure 4. EDX elemental line scans for Mn:GaN nanowires with (a) hexagonal and (b) triangular cross sections. The insets are TEM images of the respective nanowires; the dashed horizontal lines correspond to the positions at which the EDX line scans were taken. The red and green data points correspond to Ga and Mn, respectively, in both a and b. The solid lines correspond to fits as discussed in the text. The Mn profiles were multiplied by a factor of 20 for clarity.

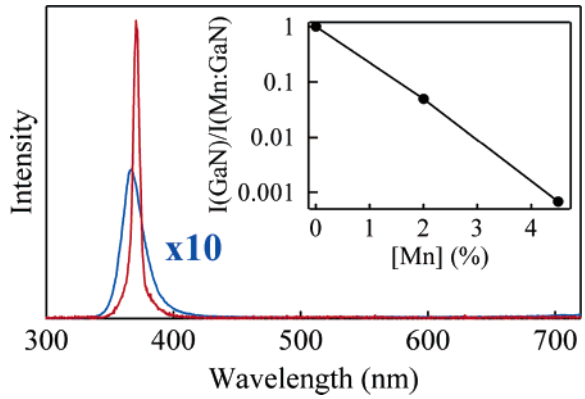

Figure 5. PL spectrum of single Mn:GaN (blue) and GaN (red) nanowires recorded at 300 K. Both nanowires were 70 nm in diameter, and the Mn concentration was 2%. (Inset) Plot of the ratio of band-edge emission intensity for GaN/Mn:GaN vs [Mn].

and triangular morphology nanowires. The nanowire diameters determined from the fits, 33 nm for the hexagonal and 230 nm for the triangular Mn:GaN nanowires, also agree with diameters determined directly from the TEM images. Hence, these results show that the Mn ions are distributed homogeously within the Mn:GaN nanowires and not localized, for example, near the surface, or segregated in separate phases.

PL studies of single Mn:GaN nanowires were carried out to further investigate the nature of the dopant ions within the GaN host lattice. Typical room-temperature PL data recorded from a Mn:GaN nanowire with ca. 2% Mn (Figure 5) show a single feature centered at 367 nm that is characteristic of GaN band-edge emission. A comparison of the PL spectra recorded from similarly sized Mn:GaN and GaN nanowires under the same conditions (Figure 5, blue vs red plots) demonstrates that emission is ca. 20× weaker in the 2% Mn-doped sample; additional data from the ca. 5% Mn-doped sample (inset, Figure 5) show a further reduction in the band-edge emission intensity. These results are consistent with the quenching of band-edge emission by the Mn dopant ions, although no spectral features characteristic of the $^4T_1 \rightarrow {}^6A_1$ transition in tetrahedral Mn^{2+} are observed, in contrast to the situation for the Mn-doped CdS and ZnS nanowires. The band-edge emission decreases exponentially with Mn dopant concentration (inset, Figure 5). This dependence is substantially stronger than that observed for the Mn:CdS and Mn:ZnS nanowires, although strong PL quenching has also been reported in Mn-doped GaN thin films prepared by molecular beam epitaxy.[29] In the future, we believe that the physical origin of this interesting behavior can be resolved by carrying out both time-resolved and steady-state PL measurements on these Mn:GaN nanowires and on samples modified, for example, by annealing.

Emission quenching by manganese in Mn:GaN materials has been attributed to different mechanisms. Emission quenching in well-characterized Mn:GaN thin films grown by molecular beam epitaxy has been attributed to the presence of a deep Mn^{3+} neutral state that facilitates nonradiative recombination of band-edge electrons and holes.[29] These results are similar to our observations of quenching of band-edge emission and contrast with recent studies of Mn:GaN nanowires prepared using carbon nanotube templates where spectral features were assigned to the $^4T_1 \rightarrow {}^6A_1$ transition in tetrahedral Mn^{2+}. This difference with our work could be explained by Mn incorporation in the near surface region or secondary phases in the previous work[12] and not in bulk GaN lattice sites, and underscores the importance of careful composition characterization needed to develop a robust understanding of the physical properties of these new materials.

In summary, we have demonstrated a general approach for the synthesis of manganese-doped II−VI and III−V nanowires based on metal nanocluster-catalyzed CVD. TEM, HRTEM, and EDX measurements have shown that the Mn-doped CdS, ZnS, and GaN nanowires, which have controllable manganese concentration, are single-crystalline structures and homogeneously doped with no evidence of secondary phases. PL measurements of individual Mn-doped CdS and ZnS nanowires show characteristic pseudo-tetrahedral Mn^{2+} ($^4T_1 \rightarrow {}^6A_1$) transitions, whereas PL studies of Mn-doped GaN nanowires suggest that manganese is incorporated as a neutral deep Mn^{3+} state. The general and controlled synthesis of nanowires doped with magnetic metal ions opens up opportunities for fundamental studies of optical, electrical, and magnetic properties in quasi-1D DMS systems and could lead to the development of nanoscale spintronic devices.

Acknowledgment. We thank R. Agarwal, O. Hayden, Y. Wu, and W. Lu for helpful discussions and A. J. Garratt-Reed (MIT) for assistance with TEM/EDX measurements. C.M.L. acknowledges the support of this work by the Air Force Office of Scientific Research.

Supporting Information Available: TEM analysis of Mn-doped ZnS. EDX line scan data and simulations for Mn-doped CdS. This material is available free of charge via the Internet at http://pubs.acs.org.

References

(1) Hu, J.; Odom, T. W.; Lieber, C. M. *Acc. Chem. Res.* **1999**, *32*, 435. Lieber, C. M. *Sci. Am.* **2001**, *September*, 58. Lieber, C. M. *MRS Bull.* **2003**, *28*, 486.

(2) Samuelson, L. *Mater. Today* **2003**, *6*, 22. Xia, Y.; Yang, P.; Sun, Y.; Wu, Y.; Mayers, B.; Gates, B.; Yin, Y.; Kim, F.; Yan, H. *Adv. Mater.* **2003**, *15*, 353. Wang, Z. L. *Mater. Today* **2004**, *7*, 26.

(3) Cui, Y.; Wei, Q.; Park, H.; Lieber, C. M. *Science* **2001**, *293*, 1289. Patolsky, F.; Lieber, C. M. *Mater. Today* **2005**, *8*, 20.

(4) Duan, X.; Huang, Y.; Cui, Y.; Wang, J.; Lieber, C. M. *Nature* **2001**, *409*, 66. Gudiksen, M.; Lauhon, L.; Wang, J.; Smith, D.; Lieber, C. M. *Nature* **2002**, *415*, 617. Huang, Y.; Duan, X.; Lieber, C. M. *Small* **2005**, *1*, 142.

(5) Zhong, Z.; Qian, F.; Wang, D.; Lieber, C. M. *Nano Lett.* **2003**, *3*, 343.

(6) Furdyna, J. K.; Kossut, J., Eds. *Diluted Magnetic Semiconductors*; Academic Press: New York, 1988; Vol. 25.

(7) Pearton, S. J.; Abernathy, C. R.; Overberg, M. E.; Thaler, G. T.; Norton, D. P.; Theodoropoulou, N.; Hebard, A. F.; Park, Y. D.; Ren, F.; Kim, J.; Boatner, L. A. *J. Appl. Phys.* **2003**, *93*, 1.

(8) Wolf, S. A.; Awschalom, D. D.; Buhrman, R. A.; Daughton, J. M.; von Molnar, S.; Roukes, M. L.; Chtchelkanova, A. Y.; Treger, D. M. *Science* **2001**, *294*, 1488.

(9) Mikulec, F. V.; Kuno, M.; Bennati, M.; Hall, D. A.; Griffin, R. G.; Bawendi, M. G. *J. Am. Chem.* Soc. **2000**, *122*, 2532.

(10) Radovanovic, P. V.; Gamelin, D. R. *J. Am. Chem. Soc.* **2001**, *123*, 12207.

(11) Norris, D. J.; Yao, N.; Charnock, F. T.; Kennedy, T. A. *Nano Lett.* **2001**, *1*, 3.

(12) Deepak, F. L.; Vanitha, P. V.; Govindaraj, A.; Rao, C. N. R. *Chem. Phys. Lett.* **2003**, *374*, 314.

(13) Ronning, C.; Gao, P. X.; Ding, Y.; Wang, Z. L. *Appl. Phys. Lett.* **2004**, *84*, 783.

(14) Han, D. S.; Park, J.; Rhie, K. W.; Kim, S.; Chang, J. *Appl. Phys. Lett.* **2005**, *86*, 032506.

(15) Barrelet, C. J.; Wu, Y.; Bell, D. C.; Lieber, C. M. *J. Am. Chem. Soc.* **2003**, *125*, 11498.

(16) Mn-doped NWs were suspended in ethanol, dispersed on a lacey carbon copper grid, and imaged using high-resolution TEM (JEOL 2010F). Elemental composition and elemental line scan profiles were determined by EDX spectroscopy in the scanning TEM mode. Photoluminescence measurements were performed on single nanowires with home-built far-field epifluorescence microscopes using charged-coupled device (CCD) cameras as the detectors. CdS NWs were optically excited at 395 nm with a frequency-doubled Ti: sapphire laser, whereas ZnS and GaN NWs were excited at 266 nm with a frequency-quadrupled Nd:YVO_4 laser system.

(17) De Boeck, J.; Oesterholt, R.; Van Esch, A.; Bender, H.; Bruynseraede, C.; Van Hoff, C.; Borghs, G. *Appl. Phys. Lett.* **1996**, *68*, 2744. Wellmann, P. J.; Garcia, J. M.; Feng, J.-L.; Petroff, P. M. *Appl. Phys. Lett.* **1997**, *71*, 2532.

(18) The model assumes a cylindrical nanowire cross section and negligible X-ray reabsorption and takes into account the Gaussian electron probe profile of the 2.5 nm full-width at half-maximum. For the triangular GaN nanowire, a geometrical model having a triangular cross section defined by three 60° angles was used, where the orientation relative to the electron beam was adjusted as described previously.[20]

(19) Lauhon, L. J.; Gudiksen, M. S.; Wang, D.; Lieber, C. M. *Nature* **2002**, *420*, 57. Gudiksen, M. S. Ph.D. Thesis, Harvard University, Cambridge, MA, 2002.

(20) Qian, F.; Li, Y.; Gradečak, S.; Wang, D.; Barrelet, C. J.; Lieber, C. M. *Nano Lett.* **2004**, *4*, 1975.

(21) Ingrey, S. J.; Shepherd, F. R.; Westwood, W. D. *J. Vac. Sci. Technol.* **1980**, *17*, 481.

(22) Duan, X.; Huang, Y.; Agarwal, R.; Lieber, C. M. *Nature* **2003**, *421*, 242.

(23) Ehrlich, C.; Busse, W.; Gumlich, H.-E.; Tschierse, D. *J. Cryst. Growth* **1985**, *72*, 371.

(24) Langer, D. W.; Richter, H. J. *Phys. Rev.* **1966**, *146*, 554.

(25) Kanemitsu, Y.; Matsubara, H.; White, C. W. *Appl. Phys. Lett.* **2002**, *81*, 535.

(26) Lever, A. B. P. *Inorganic Electronic Spectroscopy*, 2nd ed.; Elsevier: Amsterdam, 1984; pp 448−449 and references therein.

(27) Langer, D.; Ibuki, S. *Phys. Rev.* **1965**, *138*, A809.

(28) Dietl, T.; Ohno, H.; Matsukura, F.; Cibet, J.; Ferrand, D. *Science* **2000**, *287*, 1019.

(29) Gelhausen, O.; Malguth, E.; Phillips, M. R.; Goldys, E. M.; Strassburg, M.; Hoffmann, A.; Graf, T.; Gjukic, M.; Stutzmann, M. *Appl. Phys. Lett.* **2004**, *84*, 4514.

NL050747T